

Deep Convolutional Neural Networks for Lesion Detection in Digital Mammograms

Kheira Belarbi ^{1*}, Abderrahim Belmadani ²

¹Ph.D. student, Department of Computer Science, Faculty of Mathematics and Computer Science, University of Science and Technology of Oran Mohamed Boudiaf (USTO-MB), Oran, Algeria

²Professor, Department of Computer Science, Faculty of Mathematics and Computer Science, University of Science and Technology of Oran Mohamed Boudiaf (USTO-MB), Oran, Algeria

*Corresponding Author: Kheira.belarbi@univ-usto.dz

ARTICLE INFO

Received: 30 Dec 2024

Revised: 12 Feb 2025

Accepted: 26 Feb 2025

ABSTRACT

Early detection of breast cancer significantly improves treatment outcomes and patient survival rates. This study proposes a deep learning framework for classifying benign and malignant breast lesions using the curated CBIS-DDSM dataset. The preprocessing pipeline includes three key steps: Gaussian filtering for noise reduction, CLAHE-based contrast enhancement to improve lesion visibility, and extensive data augmentation to promote generalization. We systematically evaluate three transfer learning-based CNN architectures (InceptionV3, EfficientNetBo, and MobileNetV2) initialized with ImageNet weights and fine-tuned for binary classification. Experimental results show that InceptionV3 achieves the best performance, reaching 90.2% accuracy, 87.1% sensitivity, 89.3% specificity, and an F1-score of 88.4% after only 70 epochs. EfficientNetBo provides a more efficient alternative with 88.3% accuracy and faster convergence, while MobileNetV2, with 86.1% accuracy and 82.4% sensitivity, is well-suited for deployment in resource-constrained environments. These results demonstrate that a well-designed preprocessing strategy combined with transfer learning can yield clinically relevant classification performance, with InceptionV3 emerging as the most balanced and reliable architecture.

Keywords: Breast cancer classification, deep learning, transfer learning, medical image preprocessing, data augmentation, CNN architectures.

INTRODUCTION

Breast cancer continues to be one of the most significant global health challenges for women, with millions of new cases diagnosed annually [1]. As the primary screening modality for early detection, digital mammography plays a crucial role in improving patient outcomes. However, the interpretation of mammograms presents notable difficulties, including variability in radiologist assessments and reduced sensitivity in dense breast tissue [2]. These limitations have driven the development of computer-aided diagnosis (CAD) systems to support clinical decision-making.

Recent advances in deep learning have transformed medical image analysis, with convolutional neural networks (CNNs) demonstrating particular promise for mammography interpretation. The success of these approaches stems from their ability to automatically learn discriminative features directly from image data, overcoming the constraints of traditional hand-crafted feature extraction methods [3]. Transfer learning has further enhanced this capability by enabling the adaptation of models pretrained on large natural image datasets to the specialized domain of medical imaging, even with limited annotated examples [4].

Several studies have demonstrated the potential of deep learning, particularly convolutional neural networks (CNNs), in improving breast cancer detection from mammographic images [5–7]. For instance, a two-stage deep learning pipeline was applied for automatic mass segmentation from full mammograms without user intervention [8]. In [9], a deep learning system was developed to classify breast lesions as malignant or non-malignant using both region-of-

interest patches and whole images. A method based on Faster-RCNN and transfer learning was proposed in [10] for lesion localization in breast ultrasound images. A multi-view mammogram classification model combining Transformer and multiplex convolutions was introduced in [11]. In [12], transfer learning using pre-trained deep networks was employed for lesion characterization. An automated multi-scale end-to-end neural network addressing small lesion detection was proposed in [13], while [14] introduced an ensemble of CNNs for breast cancer diagnosis. These advances have significantly improved breast cancer detection, with CNNs and transfer learning proving highly effective in medical image analysis [15–17]. However, challenges remain, particularly in ensuring standardized preprocessing and enabling fair comparisons between architectures under consistent evaluation protocols.

In this paper, we develop a CNN-based binary classification system using transfer learning to distinguish malignant from benign breast lesions in mammograms from the CBIS-DDSM dataset. Addressing the computational complexity caused by scale differences between full mammograms and small abnormalities, we focus on annotated regions of interest (ROIs) to concentrate analysis on diagnostically relevant areas. Our methodology includes a preprocessing phase and a CNN model-building phase based on three architectures: InceptionV3, EfficientNetBo, and MobileNetV2. This approach aims to provide radiologists with an efficient diagnostic tool that combines targeted ROI analysis with robust deep learning techniques for improved clinical decision-making.

METHODS

Dataset

In this study, we used the CBIS-DDSM dataset [18], a curated subset of DDSM [19], which contains 3,061 mammograms across 1,566 patient cases. Each case includes both cranio-caudal (CC) and medio-lateral oblique (MLO), with annotations identifying lesions as benign or malignant. Figure 1. provides an overview of the various types of mammographic images included in the dataset.

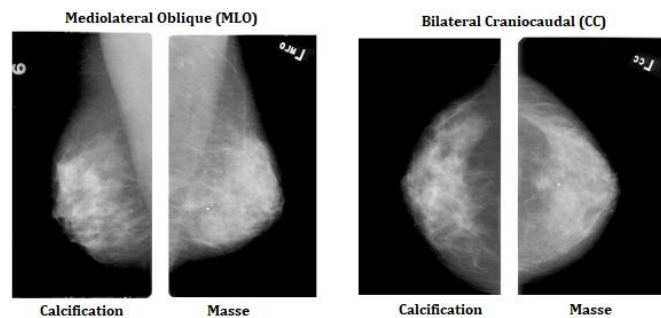


Fig1. Types of Mammographic Views in the CBIS-DDSM Dataset

The CBIS-DDSM dataset includes digitized mammography cases converted to DICOM format and reviewed by expert radiologists. It comprises two primary lesion types: masses and calcifications. In this work, we utilize the pre-extracted lesion patches provided by the dataset. These patches have been annotated and cropped by radiologists around regions of interest (ROIs), and are labeled as benign or malignant based on pathology-confirmed diagnoses. The dataset includes approximately 3,567 cropped ROI images, 3,247 ROI masks, and 2,857 full mammogram images.

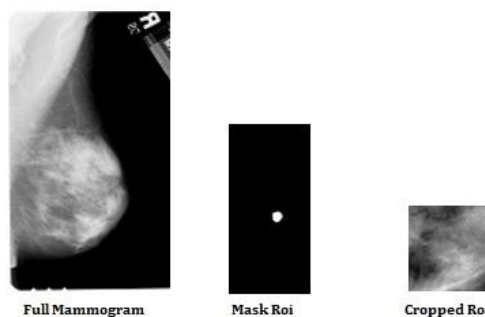


Fig 2. Examples of image types in the CBIS-DDSM Dataset

Some samples contain missing data, particularly in the ROI–full-view image pairs, with around 566 entries affected. CBIS-DDSM is widely adopted for developing and evaluating deep learning-based computer-aided diagnosis (CAD) systems for breast cancer detection. As shown in Figure 2, the CBIS-DDSM dataset comprises various image types, highlighting the range of mammographic views and corresponding annotations that support comprehensive breast cancer analysis.

Data pre-processing

Mammographic images are generally affected by noise, low contrast, and irrelevant background information, which can hinder the performance of deep learning models. Therefore, a preprocessing stage is essential to enhance image quality and highlight relevant diagnostic features before classification. The preprocessing pipeline consists of three stages:

- Gaussian filtering (3×3 kernel, $\sigma=1.0$) for noise reduction while preserving diagnostic features such as spiculated margins and microcalcification clusters;
- Contrast enhancement using CLAHE (clip limit=2.0, 8×8 tile grid) to improve visibility of subtle lesions in dense tissue;
- Data augmentation during training, including random rotations ($\pm 15^\circ$), horizontal/vertical flipping (applied with 50% probability), scaling (80-120% of original size), and translations ($\pm 10\%$ along both axes), all while maintaining pathological validity.

All ROI patches were resized to 224×224 pixels via bicubic interpolation and normalized to $[0,1]$ by dividing pixel values by 255. This standardized approach ensures optimal feature extraction while preserving clinically relevant image characteristics, as confirmed through consultation with breast radiologists.

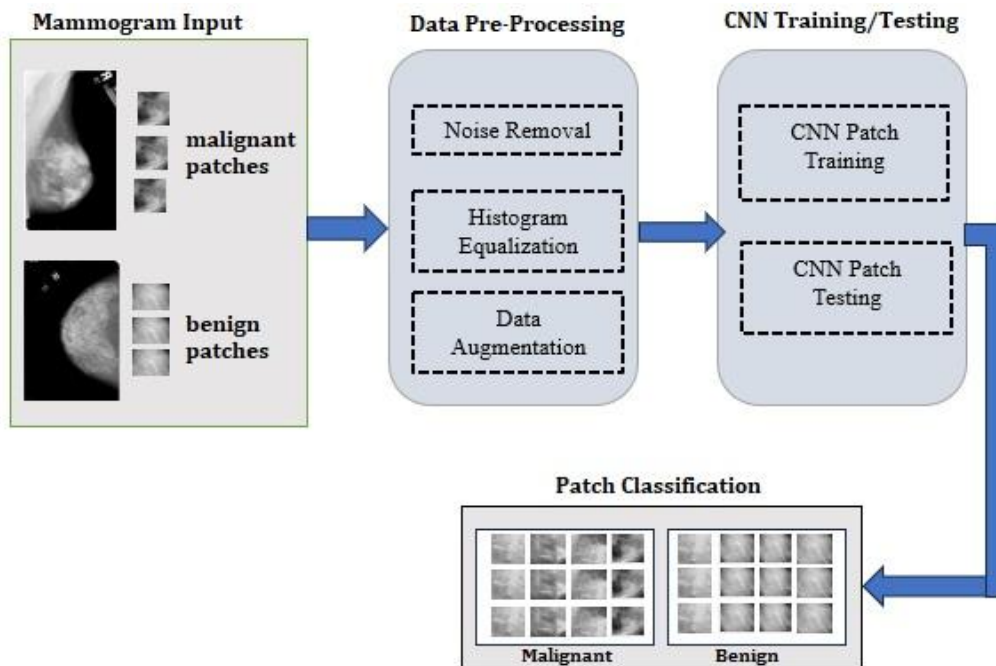


Fig 3. Overview of the classification pipeline. Malignant and benign patches are extracted from the CBIS-DDSM dataset and undergo preprocessing steps, including noise removal, histogram equalization, and data augmentation. The preprocessed patches are then used for training and testing convolutional neural networks (CNNs). The trained models classify each patch into one of two categories: benign or malignant.

CNN architectures

To address the binary classification of breast lesions, we employed three widely recognized deep convolutional neural network architectures: InceptionV3, EfficientNetBo, and MobileNetV2. These architectures were originally trained on the large-scale ImageNet dataset and have demonstrated strong performance across various visual recognition

tasks, with particular advantages in computational efficiency and multi-scale feature learning. Leveraging their powerful feature extraction capabilities, we applied transfer learning to adapt these models to the medical imaging domain, particularly for digital mammograms. For this purpose, we replaced the final classification layers of each architecture with a new fully connected head tailored to our binary classification task, distinguishing between benign and malignant lesions. This strategy allows the networks to reuse learned visual features while focusing on mammography-specific patterns during fine-tuning.

Inception-v3

The Inception-V3 [20] employs parallel convolutional pathways with different kernel sizes (1×1 , 3×3 , 5×5) within modular blocks, enabling efficient multi-scale feature extraction. The architecture stacks these Inception modules between conventional convolutional and pooling layers, using batch normalization for stable training. Its design reduces computational cost while maintaining discriminative power through hierarchical feature combination, making it suitable for detecting lesions at varying scales in mammograms. The network concludes with global pooling and fully connected layers for classification.

EfficientNetBo

The EfficientNetBo [21] optimizes model scaling through balanced adjustments of depth, width, and resolution. Its core consists of mobile inverted bottleneck blocks (MBCConv) featuring depthwise separable convolutions and channel attention mechanisms. These blocks process features at different abstraction levels while maintaining parameter efficiency. The architecture begins with a stem convolution and ends with standard classification layers, achieving high accuracy with relatively low computational requirements, which is advantageous for medical image analysis tasks.

MobileNetV2

The MobileNetV2 [22] utilizes inverted residual blocks with linear bottlenecks to create a lightweight architecture. Each block expands channel dimensions for feature processing via depthwise convolutions before projecting back to lower dimensions. This design minimizes memory usage while preserving important spatial information. The network's emphasis on efficient depthwise operations and reduced activation dimensions makes it particularly suitable for deployment in resource-constrained clinical environments requiring real-time lesion detection.

CNN TRAINING

In this study, we focused on the analysis of abnormalities within cropped regions of interest (ROIs) extracted from the CBIS-DDSM dataset, without relying on the entire mammogram. These ROI-cropped images, which represent localized lesions such as masses and calcifications, were selected based on their predominance in the SeriesDescription field. Each ROI was resized to 250×250 pixels to ensure uniform input dimensions. Since the original mammographic images are in grayscale (single-channel), each patch was replicated across the three RGB channels to meet the input requirements ($224 \times 224 \times 3$) of the CNN architectures pre-trained on the ImageNet dataset. The dataset was divided into 70% training, 15% validation, and 15% test sets, with class balance maintained across all splits. This resulted in 2,676 ROI-cropped images used for training, while 336 were reserved for testing. The remaining validation set was used to monitor generalization during training. Each image was labeled as either benign or malignant, regardless of whether the lesion type was a mass or a calcification. Before training, all input patches underwent intensity normalization to ensure consistent preprocessing across the dataset.

To train the CNNs, the dataset was divided into training and validation subsets. The training subset was used to optimize the network's parameters, while the validation subset served to assess the model's generalization capability after each epoch. To prevent overfitting and enhance the diversity of the training data, several clinically valid data augmentation techniques detailed in Section 2.2 were dynamically applied during training. These transformations modified lesion orientation, scale, and position, thereby increasing data variability and improving the model's robustness.

PACH CLASSIFICATION

After training the CNN models on the ROI-cropped patches, the classification stage aims to determine whether each localized lesion corresponds to a benign or malignant abnormality. Normal cases were not included in this study, so the classification problem was framed as a binary task, regardless of the lesion subtype (mass or calcification). Each patch was passed through the trained CNN, which produced a probability distribution over the two classes. The final label was assigned based on the higher predicted probability.

The evaluation was carried out on a held-out test set composed of 336 ROI-cropped images, equally divided between benign and malignant cases to ensure a balanced and fair assessment of model performance. The CNN models, trained using the deep features learned from the CBIS-DDSM dataset, demonstrated the ability to capture complex imaging cues and subtle variations in lesion appearance, contributing to more reliable classification.

This approach enables automated analysis of localized breast lesions, offering a practical solution for assisting radiologists in clinical diagnosis. Figure 3 illustrates the binary classification pipeline employed in this work, which includes both training on ROI-cropped images and predicting their corresponding labels.

EVALUATION METRICS

To assess the performance of our CNN models in classifying breast lesions, we employed four key metrics calculated from the confusion matrix (True Positives TP, False Positives FP, True Negatives TN, False Negatives FN):

Accuracy: Measures overall correctness of predictions.

$$Accuracy = \frac{TP + TN}{TP + TN + FP + FN} \quad (1)$$

Sensitivity (Recall): Evaluates the model's ability to detect malignant cases.

$$Sensitivity = \frac{TP}{TP + FN} \quad (2)$$

Specificity: Assesses correctness in identifying benign cases.

$$Specificity = \frac{TN}{TN + FP} \quad (3)$$

F1-Score: Balances precision and recall (harmonic mean).

$$F1 - score = 2 \times \frac{Precision \times Recall}{Precision + Recall}, \text{ where } Precision = \frac{TP}{TP + FP} \quad (4)$$

These metrics provide complementary insights: Accuracy for overall performance, Sensitivity/Specificity for class-wise reliability, and F1-Score for imbalanced data robustness.

RESULTS AND DISCUSSION

All experiments were conducted using Google Colaboratory with GPU acceleration, leveraging TensorFlow and Keras frameworks to optimize computational efficiency. The full pipeline includes three-stage image enhancement, patch extraction, and progressive fine-tuning. We evaluated three CNN architectures (InceptionV3, EfficientNetBo, and MobileNetV2) on preprocessed ROI-cropped patches from the CBIS-DDSM dataset. Transfer learning was employed by initializing each model with ImageNet pre-trained weights, while fine-tuning was restricted to the top classification layers for the binary classification task. The training protocol standardized input dimensions (224×224 pixels for MobileNetV2 and EfficientNetBo, 299×299 for InceptionV3) and incorporated data augmentation through clinically valid transformations (e.g., rotations, flips, and scaling) as detailed in Section 2.2 to enhance generalization. Models were trained for up to 150 epochs with a batch size of 32, using the Adam optimizer (initial learning rate 1e-3) and binary cross-entropy loss, while implementing early stopping (patience=15 epochs) and learning rate reduction on plateau (factor=0.1, patience=5) to prevent overfitting and optimize convergence. The dataset was partitioned into 70% training, 15% validation, and 15% test sets with balanced class distribution, with all experiments

ensuring reproducibility through fixed random seeds (42) and hardware efficiency via mixed-precision training. Figure 4 illustrates the comparative training dynamics, while Table 1 summarizes performance metrics.

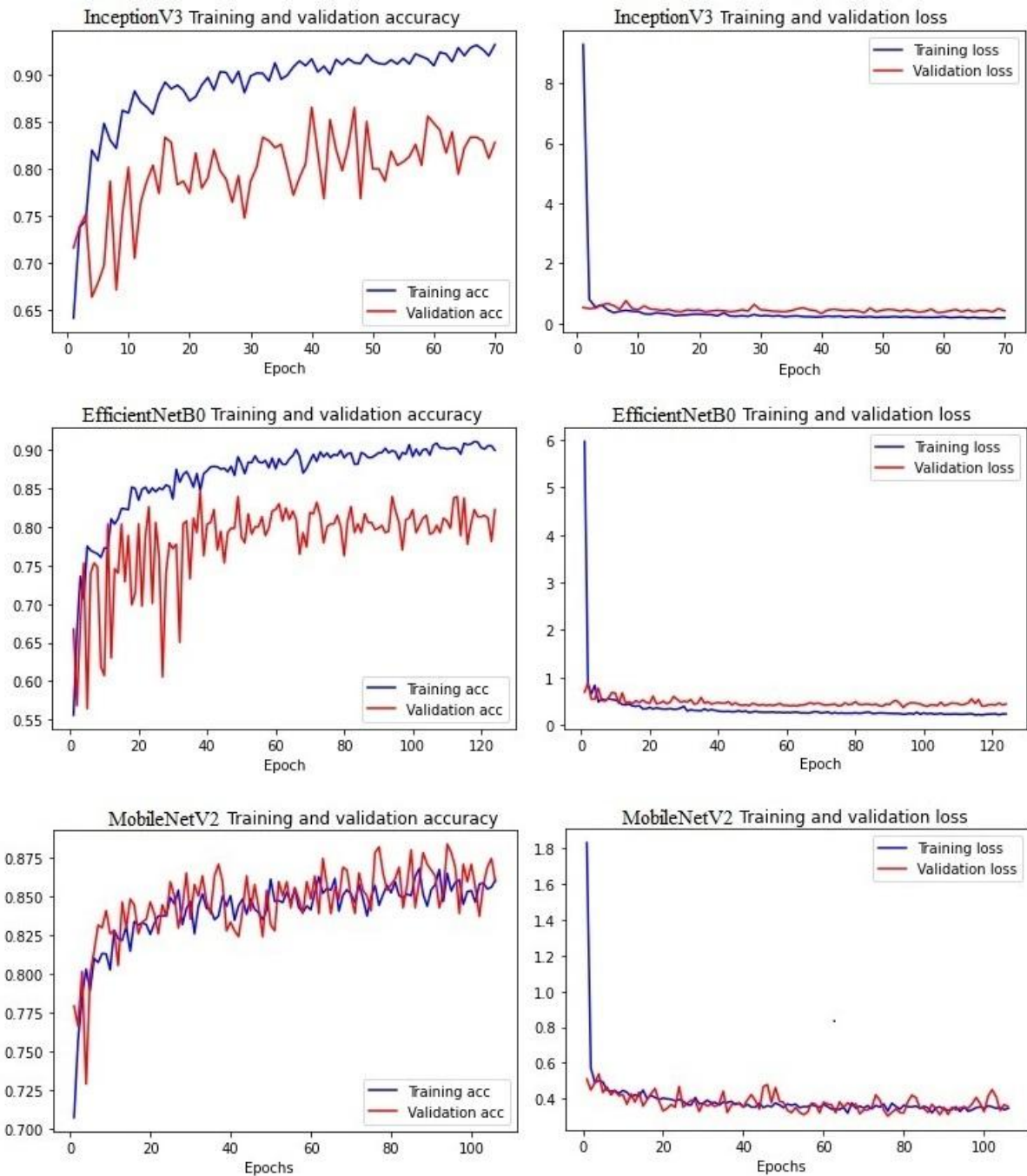


Fig 4. Training dynamics of transfer learning models: InceptionV3, EfficientNetB0, and MobileNetV2, showing accuracy and loss evolution across epochs

InceptionV3: The figure demonstrates that InceptionV3 achieves a validation accuracy of 90% after 70 epochs, with the final loss stabilizing around 0.25. The learning curve indicates progressive convergence without significant overfitting, attributable to data augmentation and fine-tuning (transfer learning). The sensitivity (87%) and specificity (89%) confirm its robust capability to discriminate between malignant and benign lesions. InceptionV3's deep architecture can explain these superior performance metrics, which effectively capture hierarchical complex features.

EfficientNetBo: EfficientNetBo exhibits a validation accuracy of 88% with a final loss of 0.30, achieved within 100 epochs. Both accuracy and loss curves demonstrate stable optimization through transfer learning. While slightly less accurate than InceptionV3, this model provides an excellent balance between performance and computational efficiency, as evidenced by its F1-Score (85%). Its specificity (87%) makes it particularly reliable for minimizing false positives - a crucial advantage in clinical diagnostics.

MobileNetV2: With a validation accuracy of 86% and final loss of 0.35 after 100 epochs, MobileNetV2 emerges as the lightest but least performant among the three architectures. Its relatively lower sensitivity (82%) suggests a higher false negative rate, which may limit its application in demanding clinical scenarios. However, its operational speed and low memory footprint render it a viable option for embedded or real-time deployment systems.

Overall, InceptionV3 emerged as the best-performing model, achieving the highest accuracy, sensitivity, and specificity across all experiments, making it the most reliable architecture for lesion classification in the CBIS-DDSM dataset. EfficientNetBo offered a compelling trade-off between accuracy and computational cost, while MobileNetV2, although the least accurate, demonstrated the fastest inference times, suggesting its potential suitability for deployment in resource-constrained or real-time diagnostic settings. These results highlight the critical balance between performance and efficiency when selecting models for clinical use.

Table 1. Comparative performance of deep learning architectures for breast lesion classification

Model	Accuracy(%)	Sensitivity (%)	Specificity (%)	F1-Score (%)
InceptionV3	90.2	87.1	89.3	88.4
EfficientNetBo	88.3	85.2	87.5	85.2
MobileNetV2	86.1	82.4	85.8	83.7

The quantitative evaluation in Table 1 demonstrates that all three transfer learning models successfully classified breast lesions, with InceptionV3 emerging as the most robust architecture. The model attained the highest accuracy (90.2%) and F1-score (88.4%), coupled with balanced sensitivity (87.1%) and specificity (89.3%), indicating its clinical reliability for minimizing both false positives and negatives. EfficientNetBo followed closely with 88.3% accuracy and 85.2% F1-score, showing particular strength in specificity (87.5%) that makes it suitable for scenarios prioritizing false positive reduction. MobileNetV2, while slightly less performant (86.1% accuracy, 83.7% F1-score), maintained reasonable sensitivity (82.4%) and specificity (85.8%), suggesting its potential for resource-constrained implementations where moderate performance trade-offs are acceptable. Notably, all models exceeded 85% specificity, confirming their effectiveness in correctly identifying benign lesions, which is a critical requirement for clinical decision support systems. The performance hierarchy (InceptionV3 > EfficientNetBo > MobileNetV2) remained consistent across all metrics, validating the comparative analysis of their training dynamics shown in Figure 4.

Table 2. Comparative results with existing methods

Reference	Approach	Model	Accuracy(%)
[23]	Transfer Learning	VGG16	83.10
[24]	Transfer Learning	AlexNet VGG16	90.87 86.52
[25]	Classical Machine Learning	Naive Bayes classifier	83.00
[26]	Deep Learning-based	CNN + Multi-Layer Perceptron (MLP)	80.00
Ours	Transfer Learning with CNNs	InceptionV3	90.20
		EfficientNetBo	88.30
		MobileNetV2	86.10

To validate the effectiveness of our transfer learning-based approach, we compared the performance of three deep convolutional architectures, InceptionV3, EfficientNetBo, and MobileNetV2, with existing methods applied on the CBIS-DDSM dataset for the classification of benign and malignant breast tumors; the comparative results are shown in Table 2. In [23], the VGG16 model achieved an accuracy of 83.1%, while in [24], AlexNet reached 90.87% and VGG16 obtained 86.52%. The classical Naive Bayes classifier reported in [25] achieved 83%, and the CNN combined with MLP in [26] reached 80%. In comparison, our models achieved 90.2% with InceptionV3, 88.3% with EfficientNetBo, and 86.1% with MobileNetV2, demonstrating superior overall performance and greater robustness for classifying breast lesions on the CBIS-DDSM dataset.

CONCLUSION

We proposed a deep convolutional neural network (CNN) approach for early-stage breast cancer lesion detection using the CBIS-DDSM dataset. Our framework integrates image preprocessing, data augmentation, and transfer learning to achieve high classification performance. This approach shows strong potential for deployment in clinical CAD systems. Among the tested architectures, InceptionV3 demonstrated the most consistent and balanced results, particularly in sensitivity and F1-score, highlighting its suitability for medical imaging tasks involving subtle lesion features. While all models benefited from the standardized preprocessing pipeline, the results also reflected the common trade-offs between sensitivity and specificity, crucial considerations in clinical decision-making. Future work will focus on integrating attention mechanisms and hybrid architectures to further improve diagnostic accuracy.

This study underscores the effectiveness of deep CNNs in distinguishing benign from malignant breast lesions in mammographic images. The exclusive use of the CBIS-DDSM dataset provides a focused and clinically relevant benchmark. Moreover, the preprocessing techniques significantly enhanced image quality, facilitating better model convergence. Overall, our findings suggest that CNN-based CAD systems can provide radiologists with reliable second opinions, potentially reducing false diagnoses and improving patient outcomes.

REFERENCES

- [1] Sung, H., Ferlay, J., Siegel, R. L., Laversanne, M., Soerjomataram, I., Jemal, A., & Bray, F. (2021). Global cancer statistics 2020: GLOBOCAN estimates of incidence and mortality worldwide for 36 cancers in 185 countries. *CA: A Cancer Journal for Clinicians*, 71(3), 209–249. doi: <https://doi.org/10.3322/caac.21660>
- [2] Magny, S. J., Shikhman, R., & Keppke, A. L. (2023, August 28). Breast Imaging Reporting and Data System. In *StatPearls*. StatPearls Publishing. doi: <https://www.ncbi.nlm.nih.gov/books/NBK470401/>
- [3] Litjens, G., et al. (2017). A survey on deep learning in medical image analysis. *Medical Image Analysis*, 42, 60–88. doi: <https://doi.org/10.1016/j.media.2017.07.005>
- [4] Yosinski, J., Clune, J., Bengio, Y., & Lipson, H. (2014). How transferable are features in deep neural networks? In *Advances in Neural Information Processing Systems* (Vol. 27, pp. 3320–3328). doi: <https://doi.org/10.48550/arXiv.1411.1792>
- [5] Shen, L., Margolies, L. R., Rothstein, J. H., Fluder, E., McBride, R., & Sieh, W. (2019). Deep learning to improve breast cancer detection on screening mammography. *Scientific Reports*, 9, 12495. doi: <https://doi.org/10.1038/s41598-019-48995-4>
- [6] Sarvamangala, D. R., & Kulkarni, R. V. (2022). Convolutional neural networks in medical image understanding: A survey. *Evolutionary Intelligence*, 15, 1–22. doi: <https://doi.org/10.1007/s12065-020-00540-3>.
- [7] Celard, P., Iglesias, E. L., Sorribes-Fdez, J. M., & al. (2023). A survey on deep learning applied to medical images: From simple artificial neural networks to generative models. *Neural Computing and Applications*, 35(4), 2291–2323. doi: <https://doi.org/10.1007/s00521-022-07953-4>
- [8] Yan, Y., Conze, P.-H., Quellec, G., Lamard, M., Cochener, B., & Coatrieux, G. (2021). Two-stage multi-scale breast mass segmentation for full mammogram analysis without user intervention. *Biocybernetics and Biomedical Engineering*, 41(2), 746–757. doi: <https://doi.org/10.1016/j.bbe.2021.03.005>
- [9] El Houby, E. M. F., & Yassin, N. I. R. (2021). Malignant and nonmalignant classification of breast lesions in mammograms using convolutional neural networks. *Biomedical Signal Processing and Control*, 70, 102954. doi: <https://doi.org/10.1016/j.bspc.2021.102954>.

- [10] Cheung, B. H. H., Co, M., Lui, T. T. N., & Kwong, A. (2024, April 15). Evolution of localization methods for non-palpable breast lesions: A literature review from a translational medicine perspective. *Translational Breast Cancer Research*, 5, 12. doi: <https://doi.org/10.21037/tbcr-23-49>.
- [11] Xia, L., An, J., Ma, C., Hou, H., Hou, Y., Cui, L., Jiang, X., Li, W., & Gao, Z. (2023). Neural network model based on global and local features for multi-view mammogram classification. *Neurocomputing*, 536, 21–29. doi: <https://doi.org/10.1016/j.neucom.2023.03.028>.
- [12] Samala, R. K., Chan, H. P., Hadjiiski, L., Helvie, M. A., Wei, J., & Cha, K. (2016, December). Mass detection in digital breast tomosynthesis: Deep convolutional neural network with transfer learning from mammography. *Medical Physics*, 43(12), 6654. doi: <https://doi.org/10.1118/1.4967345>.
- [13] Xie, L., Zhang, L., Hu, T., Huang, H., & Yi, Z. (2020). Neural networks model based on an automated multi-scale method for mammogram classification. *Knowledge-Based Systems*, 208, 106465. doi: <https://doi.org/10.1016/j.knsys.2020.106465>.
- [14] Shah, D., Khan, M. A. U., Abrar, M., & Tahir, M. (2024). Optimizing breast cancer detection with an ensemble deep learning approach. *International Journal of Intelligent Systems*, 2024, 5564649. doi: <https://doi.org/10.1155/2024/5564649>.
- [15] Kooi, T., Litjens, G., van Ginneken, B., Gubern-Mérida, A., Sánchez, C. I., Mann, R., den Heeten, A., & Karssemeijer, N. (2017). Large scale deep learning for computer aided detection of mammographic lesions. *Medical Image Analysis*, 35, 303–312. doi: <https://doi.org/10.1016/j.media.2016.07.007>.
- [16] Ribli, D., Horváth, A., Unger, Z., Pollner, P., & Csabai, I. (2018, March 15). Detecting and classifying lesions in mammograms with deep learning. *Scientific Reports*, 8(1), 4165. doi: <https://doi.org/10.1038/s41598-018-22437-z>.
- [17] Shen, L., Margolies, L. R., Rothstein, J. H., et al. (2019). Deep learning to improve breast cancer detection on screening mammography. *Scientific Reports*, 9, 12495. doi: <https://doi.org/10.1038/s41598-019-48995-4>.
- [18] Lee, R. S., Gimenez, F., Hoogi, A., Miyake, K. K., & Rubin, D. L. (2017). A curated mammography data set for use in computer-aided detection and diagnosis research. *Scientific Data*, 4, 170177. doi: <https://doi.org/10.1038/sdata.2017.177>.
- [19] Heath, M., Bowyer, K., Kopans, D., Moore, R., & Kegelmeyer, W. P. (2000). The digital database for screening mammography. In *Proceedings of the 5th International Workshop on Digital Mammography* (pp. 212–218). Medical Physics Publishing.
- [20] Szegedy, C., Vanhoucke, V., Ioffe, S., Shlens, J., & Wojna, Z. (2016). Rethinking the Inception architecture for computer vision. In *2016 IEEE Conference on Computer Vision and Pattern Recognition (CVPR)* (pp. 2818–2826). IEEE. doi: <https://doi.org/10.1109/CVPR.2016.308>
- [21] Tan, M., & Le, Q. V. (2019). EfficientNet: Rethinking model scaling for convolutional neural networks. In *Proceedings of the 36th International Conference on Machine Learning (ICML)* (Vol. 97, pp. 6105–6114). PMLR. doi: <https://doi.org/10.48550/arXiv.1905.11946>
- [22] Sandler, M., Howard, A., Zhu, M., Zhmoginov, A., & Chen, L.-C. (2018). MobileNetV2: Inverted residuals and linear bottlenecks. In *Proceedings of the 2018 IEEE/CVF Conference on Computer Vision and Pattern Recognition (CVPR)* (pp. 4510–4520). IEEE. doi: <https://doi.org/10.1109/CVPR.2018.00474>
- [23] Shen, L., Margolies, L. R., Rothstein, J. H., Fluder, E., McBride, R., & Sieh, W. (2019). Deep learning to improve breast cancer detection on screening mammography. *Scientific Reports*, 9(1), 1–12. doi: <https://doi.org/10.1038/s41598-019-48995-4>.
- [24] Gnanasekaran, V. S., Joypaul, S., Meenakshi Sundaram, P., & Chairman, D. D. (2020). Deep learning algorithm for breast masses classification in mammograms. *IET Image Processing*, 14(12), 2860–2868. doi: <https://doi.org/10.1049/iet-ipr.2020.0070>.
- [25] Suhail, Z., Hamidinekoo, A., & Zwiggelaar, R. (2018). Mammographic mass classification using filter response patches. *IET Computer Vision*, 12(8), 1060–1066. doi: <https://doi.org/10.1049/iet-cvi.2018.5244>.

- [26] Qiu, Y., Wang, Y., Yan, S., Tan, M., Cheng, S., Liu, H., & Zheng, B. (2016). An initial investigation on developing a new method to predict short-term breast cancer risk based on deep learning technology. In Medical Imaging 2016: Computer-Aided Diagnosis (Vol. 9785). SPIE. doi: <https://doi.org/10.1117/12.2217126>.